Cancellation of laser noise in an unequal-arm interferometer detector of gravitational radiation

Massimo Tinto* and J. W. Armstrong†
Jet Propulsion Laboratory, California Institute of Technology, Pasadena, California 91109
(Received 13 October 1998; published 22 April 1999)

Equal-arm interferometric detectors of gravitational radiation allow phase measurements many orders of magnitude below the intrinsic phase stability of the laser injecting light into their arms. This is because the noise in the laser light is common to both arms, experiencing exactly the same delay, and thus cancels when it is differenced at the photo detector. In this situation, much lower level secondary noises then set overall performance. If, however, the two arms have different lengths (as will necessarily be the case with space-borne interferometers), the laser noise experiences different delays in the two arms and will hence not directly cancel at the detector. In this paper we present a method for exactly canceling the laser noise in a one-bounce unequal-arm Michelson interferometer. The method requires separate measurements of the phase difference in each arm, made by interfering the returning laser light in each arm with the outgoing light. Let these two time series of phase difference be z_i, $i=1,2$. By forming the quantity $[z_1(t-2L_2/c)-z_1(t)]-[z_2(t-2L_1/c)-z_2(t)]$, where L_i are the arm lengths, gravitational wave signals remain while the laser noise is canceled. Unlike other proposed methods, this procedure accurately cancels the laser noise if the arm lengths are known. This method is direct in time and allows for time-varying arm-lengths. In this paper we demonstrate that this method precisely cancels the laser noise, present the transfer function of gravitational waves after forming this linear combination, and discuss system requirements (such as required knowledge of the arm lengths). We verify the technique with numerical simulation of periodic gravitational wave signals embedded in laser and shot noise having spectra expected for a space-borne interferometer, and compare our time-domain approach with approximate correction methods based on Fourier transforms of the z_i processes.
[S0556-2821(99)00710-9]

PACS number(s): 04.80.Nn, 07.60.Ly, 95.55.Ym

I. INTRODUCTION

Interferometric, non-resonant, detectors of gravitational radiation (with frequency content $0<f<f_H$) use a coherent train of electromagnetic waves (of nominal frequency $\nu_0 \gg f_H$) folded into several beams and, at one or more points where these intersect, monitor relative fluctuations of frequency or phase (homodyne detection). The observed low frequency signals are due to frequency variations of the source of the electromagnetic signal about ν_0, to relative motions of the source and the mirrors (or amplifying transponders) that do the folding, to temporal variations of the index of refraction along the beams, and, according to general relativity, to any time-variable gravitational fields present, such as the transverse traceless metric curvature of a passing plane gravitational wave train. To observe gravitational waves in this way, it is thus necessary to control, or monitor, the other sources of relative frequency fluctuations and, in the data analysis, to use optimal algorithms based on the different characteristic interferometer responses to gravitational waves (the signal) and to the other sources (the noise) [1]. By comparing phases of split beams propagated along non-parallel equal-length arms, frequency fluctuations of the frequency reference can be removed and gravitational wave signals at levels many orders of magnitude lower can be detected. Especially for space-based interferometers, which may use lasers with a frequency stability at best of a few parts in 10^{-13}, it is essential to be able to remove these fluctuations when searching for gravitational waves of dimensionless amplitudes less than 10^{-20} in the millihertz band [3].

In present single-spacecraft Doppler tracking observations many of the noise sources can be either reduced or calibrated by implementing appropriate microwave frequency links and by using specialized electronics; so a fundamental limitation is imposed by the frequency (time-keeping) fluctuations inherent to the reference clock that controls the microwave system. Hydrogen maser clocks, currently used in Doppler tracking experiments, achieve their best performance at about 1000 sec integration time, with a fractional frequency stability of a few parts in 10^{-16}. This is the reason why these one-arm interferometers in space (which have one detector and a ''3-pulse'' response to gravitational waves [2]) are most sensitive to millihertz gravitational waves. This integration time is also comparable to the microwave propagation (or ''storage'') time $2L/c$ to spacecraft en route to the outer solar system (for example $L\simeq 5-8$ AU for the Cassini spacecraft).

Next-generation low-frequency gravitational wave detectors, Michelson optical interferometers in Earth or solar orbits [3], have been proposed to achieve greater sensitivity to millihertz gravitational waves. Since the arm lengths of these space-based interferometers can be different by several percent, the direct recombination of the two beams at a photo detector will not however effectively remove the laser noise. This is because the frequency fluctuations of the laser will be delayed by a different amount of time inside the two different-length arms. In order to solve this problem, a tech-

*Electronic address: Massimo.Tinto@jpl.nasa.gov
†Electronic address: John.W.Armstrong@jpl.nasa.gov

nique involving heterodyne interferometry with unequal arm lengths and independent phase-difference readouts in each arm was proposed [5], which yielded data from which source frequency fluctuations were removed by several orders of magnitude. The technique discussed in [5] relied on the observation that the laser frequency fluctuations enter in the Fourier transforms of the Doppler time series, taken over an infinitely long integration time, with well-defined transfer functions. It was argued therefore that knowledge of these transfer functions would allow one to remove the frequency fluctuations of the laser by linearly combining suitably normalized Fourier transforms of the two Doppler time series. If the Fourier transform is performed, however, over a finite time interval, the analytic forms of the transfer functions of the laser fluctuations into the Fourier transforms of the Doppler responses are different from their idealized expressions valid for infinitely long integration time. Since the algorithm introduced in [5] can only be implemented for finite-length Fourier transforms of the Doppler data, only partial cancellation of the laser fluctuations can be achieved in a real experiment. The cancellation of the laser noise of course improves by increasing the integration time, and indeed becomes exact as the integration time goes to infinity. A detailed analysis of this issue is discussed in the Appendix.

In this paper we will show that it is possible to remove completely the frequency fluctuations of the laser by taking a suitable linear combination of the two Doppler time series after having time shifted them properly. This direct method achieves the exact cancellation of the laser frequency fluctuations, and does not require any Fourier transform of the data. An outline of the paper is presented below.

In Sec. II we state the problem, and derive the two Doppler responses of the two unequal arms. This implies that the frequency fluctuations of the laser cannot be removed by direct differencing of the two data sets. In Sec. III we present our technique for *synthesizing* an unequal-arm interferometer. Our method is implemented in the time domain, and relies on a properly chosen linear combination of the two Doppler data. Since our technique requires knowledge of the distances between the proof masses, estimates of the arm-length accuracies required to cancel the laser noise to a level below secondary noises are then derived. A comparison with the method introduced in Ref. [5] is discussed in the Appendix. Our comments and conclusions are finally outlined in Sec. IV.

II. STATEMENT OF THE PROBLEM

Let us consider three spacecraft flying in an equilateral triangle-like formation, each acting as a free falling test particle, and continuously tracking each other via coherent laser light. One spacecraft, which we will refer to as spacecraft *a*, transmits a laser beam of nominal frequency ν_0 to the other spacecraft (spacecrafts *b* and *c* at distances L_1 and L_2, respectively). The phase of the light received at spacecrafts *b* and *c* is used by lasers on board spacecrafts *b* and *c* for coherent transmission back to spacecraft *a*. The relative two *two-way* frequency (or phase) changes as functions of time are then independently measured at two photo detectors on board spacecraft *a* (Fig. 1). When a gravitational wave crossing the solar system propagates through these electromagnetic links, it causes small perturbations in frequency (or phase), which are replicated 3 times in each arm's data [2].

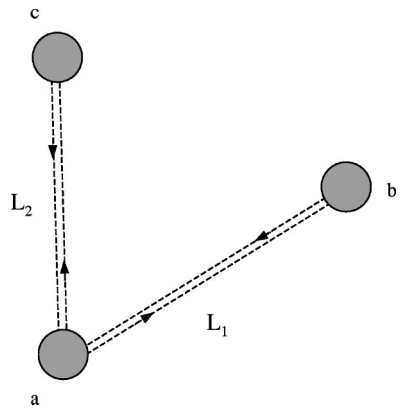

FIG. 1. Typical configuration of a space-based, unequal-arm interferometer detector of gravitational waves. The corner spacecraft *a* transmits coherent laser light to the other spacecraft, *b* and *c*. They coherently retransmit back to spacecraft *a*, where coherent two-way phase (or frequency) changes in each arm are then measured. The two arm lengths are denoted by L_1 and L_2.

To determine the response of an unequal arm interferometer to a gravitational wave pulse, let us introduce a set of Cartesian orthogonal coordinates (X,Y,Z) centered on spacecraft *a* (see Fig. 2). The *X* axis is assumed to be ori-

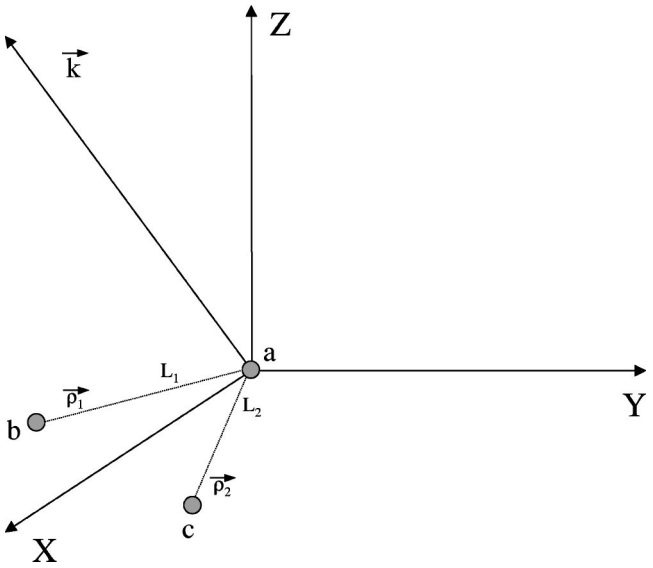

FIG. 2. Coherent laser light is transmitted simultaneously from spacecrafts *a* to spacecraft *b* and *c*, and coherently transponded back to *a*. The *X* axis is along the bisector of the angle enclosed between the two arms of the interferometer. The *Y* axis is orthogonal to the *X* axis in the plane of the interferometer, and the *Z* axis is chosen in such a way to form together with (X,Y) a right-handed set of axes. The gravitational wave train propagates along the $\vec{k}$ direction, while the unit vectors $\vec{\rho}_1$, $\vec{\rho}_2$ are along the direction of propagation of the two laser beams from spacecraft *a* to spacecraft *b* and *c* respectively. See text for a complete description.

ented along the bisector of the angle enclosed between the two arms, Y is orthogonal to it in the plane containing the three spacecraft, and the Z axis is chosen in such a way to form with (X,Y) a right-handed, orthogonal triad of axes. In this coordinate system we can write the two two-way Doppler responses, measured by spacecraft a at time t, as follows [6,7] (units in which the speed of light $c=1$):

$$\left(\frac{\Delta\nu(t)}{\nu_0}\right)_1 \equiv y_1(t) = \left[-\frac{(1-\vec{k}\cdot\vec{\rho}_1)}{2}\Psi_1(t)-\vec{k}\cdot\vec{\rho}_1 \times\Psi_1[t-(1+\vec{k}\cdot\vec{\rho}_1)L_1(t)]+\frac{(1+\vec{k}\cdot\vec{\rho}_1)}{2} \times\Psi_1[t-2L_1(t)]\right]+C[t-2L_1(t)]-C(t) +n_1(t), \tag{2.1}$$

$$\left(\frac{\Delta\nu(t)}{\nu_0}\right)_2 \equiv y_2(t) = \left[-\frac{(1-\vec{k}\cdot\vec{\rho}_2)}{2}\Psi_2(t)-\vec{k}\cdot\vec{\rho}_2 \times\Psi_2[t-(1+\vec{k}\cdot\vec{\rho}_2)L_2(t)] + \frac{(1+\vec{k}\cdot\vec{\rho}_2)}{2}\Psi_2[t-2L_2(t)]\right] +C[t-2L_2(t)]-C(t)+n_2(t), \tag{2.2}$$

where $\vec{k}$ is the unit vector in the direction of propagation of the planar gravitational wave pulse. In Eqs. (2.1), (2.2) we have denoted by $\vec{\rho}_1$, $\vec{\rho}_2$, the unit vectors from spacecraft a to spacecrafts b and c respectively; $\Psi_{(1,2)}(t)$ are the following two scalar functions:

$$\Psi_{(1,2)}(t)=\left[\frac{\rho^i_{(1,2)}\rho^j_{(1,2)}}{1-(\vec{k}\cdot\vec{\rho}_{(1,2)})^2}\right]h_{ij}(t), \tag{2.3}$$

with $h_{ij}(t)$ being the rank-2 tensor associated with the gravitational wave pulse in the (X,Y,Z) coordinate system [8], and the sum over the repeated space-like indices has been assumed. We have denoted by $C(t)$ the random process associated with the frequency fluctuations of the master laser on board spacecraft a, and $n_1(t)$, $n_2(t)$ are the remaining noise sources affecting the Doppler responses $y_1(t)$, $y_2(t)$ respectively.

From Eqs. (2.1), (2.2) it is important to note the characteristic time signature of the random process $C(t)$ in the Doppler responses y_1, y_2. The time signature of the noise $C(t)$ in $y_1(t)$, for instance, can be understood by observing that the frequency of the signal received at time t contains laser frequency fluctuations transmitted $2L_1$ seconds earlier. By subtracting from the frequency of the received signal the frequency of the signal transmitted at time t, we also subtract the frequency fluctuations $C(t)$ with the net result shown in Eq. (2.1).

Among all the noise sources included in Eq. (2.1), the frequency fluctuations due to the laser are expected to be by far the largest. A space-qualified single-mode laser, such as a diode-pumped Nd:YAG ring laser of frequency $\nu_0=3.0\times10^{14}$ Hz and phase-locked to a Fabry-Pérot optical cavity, is expected to have a spectral level of frequency fluctuations equal to about $1.0\times10^{-13}/\sqrt{\text{Hz}}$ in the millihertz band [3]. A single point frequency stability measurement performed on such a laser by McNamara *et al.* [9] indicates that a stability of about $1.0\times10^{-14}/\sqrt{\text{Hz}}$ might be achievable in the same frequency band. In this paper however we will assume the laser frequency stability mentioned in [3]. Laser noise is to be compared with, e.g., the expected secondary noises which will be 10^7 or more times smaller.

If the arm lengths are unequal by an amount $\Delta L=L_2-L_1\equiv\epsilon L_1$ (with $\epsilon\simeq3\times10^{-2}$ for a space based interferometer [3]), a simple subtraction of the two Doppler data $y_1(t)$, $y_2(t)$ gives a new data set that is still affected by the laser fluctuations by an amount equal to

$$C(t-2L_1)-C(t-2L_2)\simeq2\dot{C}(t-2L_1)\epsilon L_1. \tag{2.4}$$

As a numerical example of Eq. (2.4) we find that, at a frequency of 10^{-3} Hz and by using a laser of frequency stability equal to about $10^{-13}/\sqrt{\text{Hz}}$, the residual laser frequency fluctuations are equal to about $10^{-16}/\sqrt{\text{Hz}}$. Since the goal of proposed space-based interferometers [3] is to observe gravitational radiation at levels of $10^{-20}/\sqrt{\text{Hz}}$ or lower, it is crucial for the success of these missions to cancel laser frequency fluctuations by many more orders of magnitude.

III. ALGORITHM FOR UNEQUAL-ARM INTERFEROMETERS

In what follows we will show that there exists an algorithm in the time domain for removing the frequency fluctuations of the laser from the two Doppler data $y_1(t)$, $y_2(t)$ at any time t. This approach does not require Fourier transforms on the Doppler data. As will be shown below, this method relies only on a properly chosen linear combination of the two Doppler data in the time domain. In order to derive this technique, we will assume, for the moment, the two arm lengths L_1, L_2 to be constant and known exactly. We will remove these assumptions later, and estimate the corresponding accuracy needed in order for our technique to be still effective.

From Eqs. (2.1), (2.2) we may notice that, by taking the difference of the two Doppler data $y_1(t)$, $y_2(t)$, the frequency fluctuations of the laser now enter into this new data set in the following way:

$$\Lambda_1(t)\equiv y_1(t)-y_2(t) =h_1(t)-h_2(t)+C(t-2L_1)-C(t-2L_2) +n_1(t)-n_2(t), \tag{3.1}$$

where for simplicity of notation we have defined $h_1(t)$ and $h_2(t)$ to be the functions

$$h_1(t)=\left[-\frac{(1-\vec{k}\cdot\vec{\rho}_1)}{2}\Psi_1(t)-\vec{k}\cdot\vec{\rho}_1\Psi_1[t-(1+\vec{k}\cdot\vec{\rho}_1)L_1]+\frac{(1+\vec{k}\cdot\vec{\rho}_1)}{2}\Psi_1(t-2L_1)\right], \tag{3.2}$$

$$h_2(t)=\left[-\frac{(1-\vec{k}\cdot\vec{\rho}_2)}{2}\Psi_2(t)-\vec{k}\cdot\vec{\rho}_2\Psi_2[t-(1+\vec{k}\cdot\vec{\rho}_2)L_2]+\frac{(1+\vec{k}\cdot\vec{\rho}_2)}{2}\Psi_2(t-2L_2)\right]. \tag{3.3}$$

If we now compare how the laser frequency fluctuations enter into Eq. (3.1) against how they appear in Eqs. (2.1), (2.2), we can further make the following observation. If we time-shift the data $y_1(t)$ by the round trip light time in arm 2, $y_1(t-2L_2)$, and subtract from it the data $y_2(t)$ after it has been time-shifted by the round trip light time in arm 1, $y_2(t-2L_1)$, we obtain the following data set:

$$\begin{aligned}\Lambda_2(t)&\equiv y_1(t-2L_2)-y_2(t-2L_1)\\&=h_1(t-2L_2)-h_2(t-2L_1)+C(t-2L_1)\\&\quad-C(t-2L_2)+n_1(t-2L_2)-n_2(t-2L_1).\end{aligned} \tag{3.4}$$

In other words, the laser frequency fluctuations enter into $\Lambda_1(t)$, and $\Lambda_2(t)$ with the same time structure. This implies that, by subtracting Eq. (3.1) from Eq. (3.4), we can generate a new data set that does not contain the laser frequency fluctuations $C(t)$:

$$\begin{aligned}\Sigma(t)&\equiv\Lambda_2(t)-\Lambda_1(t)\\&=h_1(t-2L_2)-h_1(t)-h_2(t-2L_1)+h_2(t)\\&\quad+n_1(t-2L_2)-n_1(t)-n_2(t-2L_1)+n_2(t).\end{aligned} \tag{3.5}$$

From the expression of $\Lambda_2(t)$ given in Eq. (3.4), it is easy to see that the new data set $\Sigma(t)$ should be set to zero for the initial MAX$[2L_1,2L_2]$ seconds. This is because some of the data from y_1 and y_2 entering into $\Lambda_2(t)$ ''do not yet exist'' during this time interval. Since the typical round trip light time for proposed space-based laser interferometer detectors of gravitational waves will never be greater than about 33 sec [3], we conclude that the amount of data lost in the implementation of our method is negligible. Note that our procedure is different from stabilization techniques used for ground based interferometers [4].

The unequal-arm interferometer response, $\Sigma(t)$, derived in Eq. (3.5), can be rewritten explicitly, in terms of the gravitational wave functions Ψ_1, Ψ_2, as follows:

$$\begin{aligned}\Sigma(t)=&\left[\left(\frac{1-\vec{k}\cdot\vec{\rho}_1}{2}\right)\Psi_1(t)-\left(\frac{1-\vec{k}\cdot\vec{\rho}_2}{2}\right)\Psi_2(t)\right]+\left[\left(\frac{1+\vec{k}\cdot\vec{\rho}_2}{2}\right)\Psi_2(t-2L_2)-\left(\frac{1-\vec{k}\cdot\vec{\rho}_1}{2}\right)\Psi_1(t-2L_2)\right]\\&+\left[\left(\frac{1-\vec{k}\cdot\vec{\rho}_2}{2}\right)\Psi_2(t-2L_1)-\left(\frac{1+\vec{k}\cdot\vec{\rho}_1}{2}\right)\Psi_1(t-2L_1)\right]+\left[\left(\frac{1+\vec{k}\cdot\vec{\rho}_1}{2}\right)\Psi_1(t-2L_1-2L_2)-\left(\frac{1+\vec{k}\cdot\vec{\rho}_2}{2}\right)\right.\\&\left.\times\Psi_2(t-2L_1-2L_2)\right]+\vec{k}\cdot\vec{\rho}_1\Psi_1(t-(1+\vec{k}\cdot\vec{\rho}_1)L_1)-\vec{k}\cdot\vec{\rho}_2\Psi_2(t-(1+\vec{k}\cdot\vec{\rho}_2)L_2)+\vec{k}\cdot\vec{\rho}_2\Psi_2(t-2L_1-(1+\vec{k}\cdot\vec{\rho}_2)L_2)\\&-\vec{k}\cdot\vec{\rho}_1\Psi_1(t-2L_2-(1+\vec{k}\cdot\vec{\rho}_1)L_1)+n_1(t-2L_2)-n_1(t)-n_2(t-2L_1)+n_2(t).\end{aligned} \tag{3.6}$$

Equation (3.6) shows that the gravitational wave signal enters into the response of an unequal-arm interferometer at *eight* distinct times. In analogy with the terminology used for the Doppler tracking response to a gravitational wave pulse [2], we will refer to Eq. (3.6) as the *eight-pulse* response function.

It is important to point out that, as a consequence of the analytic form of the unequal-arm interferometer response given by Eq. (3.5), both the signal and the secondary noise sources will show a modulation of their power spectra. If we take the Fourier transform of Eq. (3.5), it is easy to derive the following expression for the one-sided power spectral density of $\Sigma(t)$:

$$\begin{aligned}S_\Sigma(f)\equiv&4|\tilde{h}_1(f)|^2\sin^2(2\pi fL_2)+4|\tilde{h}_2(f)|^2\sin^2(2\pi fL_1)-4\sin(2\pi fL_1)\sin(2\pi fL_2)[\tilde{h}_1(f)\tilde{h}_{2*}(f)e^{2\pi if(L_2-L_1)}\\&+\tilde{h}_{1*}(f)\tilde{h}_2(f)e^{-2\pi if(L_2-L_1)}]+4S_{n_1}(f)\sin^2(2\pi fL_2)+4S_{n_2}(f)\sin^2(2\pi fL_1),\end{aligned} \tag{3.7}$$

where the asterisk denotes complex conjugation, the two random processes n_1, n_2 have been assumed to be uncorrelated, and $S_{n_1}(f)$, $S_{n_2}(f)$ are their respective one-sided power spectral densities. Since the proposed space-based interferometer detectors

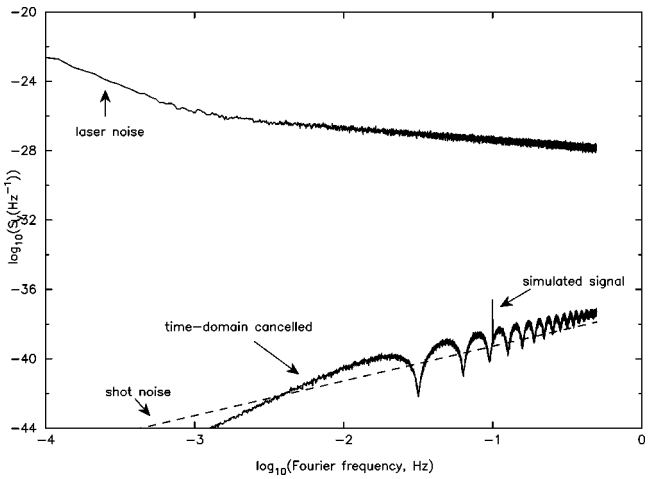

FIG. 3. Simulation of the time-domain laser noise cancellation procedure for unequal-arm interferometers described in the text. Fractional frequency fluctuation spectra, $S_y(f)$, are plotted versus Fourier frequency for (upper curve) raw laser noise having spectral density $10^{-28}(f/1\ \mathrm{Hz})^{-2/3}+6.3\times10^{-37}(f/1\ \mathrm{Hz})^{-3.4}\ \mathrm{Hz}^{-1}$ and (lower curve) residual noise after time-domain cancellation procedure. The dashed curve shows the level of shot noise added to each arm [spectral density $5.3\times10^{-38}(f/1\ \mathrm{Hz})^2\ \mathrm{Hz}^{-1}$, independent in each arm] and dot-dashed curve showing the predicted modulation of the shot noise spectrum due to our laser noise cancellation is also plotted. Other parameters were $2L_1=32$ sec, $2L_2=31$ sec, and transform length 2^{15} sec. In addition to shot noise, a simulated sinusoidal gravitational wave with amplitude $h_0=10^{-20}$ and $f_0=0.1$ Hz incident normal to the plane of the interferometer was added. The time-domain procedure, using the known arm lengths, cancels the laser noise exactly, making the simulated signal clearly visible above the (now modulated) shot noise spectrum.

will have arm lengths that will differ by up to a few percent [3], in the frequency band of interest Eq. (3.7) can be further simplified by neglecting terms of the order $f(L_2-L_1)$ and higher:

$$S_\Sigma(f)\simeq 4|\tilde{h}_1(f)-\tilde{h}_2(f)|^2\sin^2(2\pi fL_1)+4[S_{n_1}(f)+S_{n_2}(f)]\sin^2(2\pi fL_1). \quad (3.8)$$

Equation (3.8) shows that the one-sided power spectral densities of the signal and the noise display the same modulation in the Fourier domain. This result implies that the signal-to-noise ratio in an interferometer with arms that are different by a few percent is in principle equal to the signal-to-noise ratio achievable with an equal-arm detector [6].

We have simulated the procedure [Eq. (3.5)] using realistic laser and shot noise spectra [3], known arm lengths (differing by about 3%), and a simulated monochromatic gravitational wave incident normal to the plane of the interferometer. The results of the simulation are shown in Fig. 3. Plotted are spectral densities of the raw laser noise, the raw shot noise, and the canceled time series, $\Sigma(t)$ [Eq. (3.5)]. This illustrates the cancellation of the laser noise and modulation of the residual secondary noises in excellent agreement with Eq. (3.7).

By further expanding Eq. (3.8) in the long wavelength limit ($2\pi fL_1\ll1$, i.e., $f\ll10^{-2}$ Hz for a 5×10^6 km arm length), and taking into account the expressions for h_1, h_2 given by Eqs. (3.2), (3.3), (2.3), we obtain the following expression for the low-frequency response of the interferometer:

$$S_\Sigma(f)\simeq 4|(\rho_1^i\rho_1^j-\rho_2^i\rho_2^j)\tilde{h}_{ij}(f)|^2(2\pi fL_1)^4+4[S_{n_1}(f)+S_{n_2}(f)](2\pi fL_1)^2, \quad (3.9)$$

which is the response of an equal-arm, one-bounce, Michelson interferometer detector of gravitational radiation multiplied by the factor $16(2\pi fL_1)^2$ [6,8,10]. In other words the signal-to-noise ratio is the same as that of an equal-arm interferometer. For $f\geqslant10^{-3}$ Hz, most of the band to which the Laser Interferometric Space Antenna (LISA) will be sensitive [3], the 8-pulse structure will be visible.

The real limitations on the procedure described above, however, come from the remaining noise sources affecting the two Doppler data and the accuracy in the determination of the distances between the two pairs of spacecraft. We will estimate below how these errors affect the tolerance of the method. In what follows we will assume the two secondary noise random processes $n_1(t)$, $n_2(t)$ to be uncorrelated and the two arm lengths L_1, L_2 to be constant. The following analysis will identify the time scale during which the latter assumption is correct.

The derivation of our method for synthesizing an unequal-arm interferometer relied on the assumption of knowing the two arm lengths L_1, L_2 exactly. If we assume instead that the two arm lengths are known within the accuracies δL_1, δL_2 respectively, the cancellation of the laser frequency fluctuations from the data $\Sigma(t)$ is no longer exact. In order to estimate the magnitude of the laser fluctuations remaining in the data set $\Sigma(t)$, let us define $\hat{L}_1$, $\hat{L}_2$, to be the estimated arm lengths of the interferometer. They are related to the *true* arm lengths L_1, L_2 and the accuracies δL_1, δL_2 through the following expressions:

$$\hat{L}_1=L_1+\delta L_1,\qquad \hat{L}_1=L_2+\delta L_2. \quad (3.10)$$

If we now substitute Eq. (3.10) into Eqs. (3.4), (3.5), and expand Eq. (3.5) to first order in δL_1, δL_2, we find the following approximate expression for $\Sigma(t)$:

$$\Sigma(t)\simeq h_1(t-2L_2)-h_1(t)-h_2(t-2L_1)+h_2(t)+2[\dot{C}(t-2L_1-2L_2)(\delta L_1-\delta L_2)+\dot{C}(t-2L_2)(\delta L_2)-\dot{C}(t-2L_1)(\delta L_1)]+n_1(t-2L_2)-n_1(t)-n_2(t-2L_1)+n_2(t). \quad (3.11)$$

Our technique for synthesizing an unequal-arm interferometer can be considered effective if the magnitude of the remaining fluctuations from the laser are smaller than the fluctuations due to the other noise sources entering in $\Sigma(t)$. This

requirement implies an upper limit in the accuracies of the measured arm lengths. In order to estimate the magnitude of the required accuracies δL_1, δL_2, let us focus our attention on the two terms entering into Eq. (3.11), associated with the frequency fluctuations $C(t)$ and the noise sources n_1, n_2:

$$\Delta C(t) \equiv 2[\dot{C}(t-2L_1-2L_2)(\delta L_1-\delta L_2)+\dot{C}(t-2L_2)(\delta L_2) - \dot{C}(t-2L_1)(\delta L_1)], \tag{3.12}$$

$$N(t) \equiv n_1(t-2L_2)-n_1(t)-n_2(t-2L_1)+n_2(t). \tag{3.13}$$

If we denote by $\widetilde{\Delta C}(f)$, $\tilde{N}(f)$ the Fourier transforms of the random processes $\Delta C(t)$, $N(t)$ respectively, from Eqs. (3.12), (3.13) we find that they are equal to

$$\widetilde{\Delta C}(f) = 4\pi i f \tilde{C}(f) e^{4\pi i f(L_1+L_2)}[(\delta L_1-\delta L_2)+e^{-4\pi i f L_1}\delta L_2 - e^{-4\pi i f L_2}\delta L_1], \tag{3.14}$$

$$\tilde{N}(f) = 2i\tilde{n}_1(f)e^{2\pi i f L_2}\sin(2\pi f L_2) - 2i\tilde{n}_2(f)e^{2\pi i f L_1}\sin(2\pi f L_1). \tag{3.15}$$

Equations (3.14), (3.15) imply the following expressions for the one-sided power spectral densities of the noises ΔC, N:

$$S_{\Delta C}(f) = 64\pi^2 f^2 S_C(f)(\delta L_1^2 \sin^2(2\pi f L_2) + \delta L_2^2 \sin^2(2\pi f L_1) - \delta L_1 \delta L_2\{\sin^2(2\pi f L_1) + \sin^2(2\pi f L_2) - \sin^2[2\pi f(L_2-L_1)]\}), \tag{3.16}$$

$$S_N(f) = 4S_n(f)[\sin^2(2\pi f L_1)+\sin^2(2\pi f L_2)], \tag{3.17}$$

where we have assumed the two random processes n_1, n_2 to be uncorrelated, and their one-sided power spectral densities to be equal to $S_n(f)$. If the characteristic wavelength of the gravitational radiation is significantly longer than the arm lengths of the interferometer ($2\pi f L_1, 2\pi f L_2 \ll 1$), Eqs. (3.16), (3.17) can be approximated as follows:

$$S_{\Delta C}(f) \simeq 256\pi^4 f^4 S_C(f)(L_1 L_2)^2\left[\frac{\delta L_2}{L_2}-\frac{\delta L_1}{L_1}\right]^2, \tag{3.18}$$

$$S_N(f) \simeq 16\pi^2 f^2 S_n(f)[L_1^2+L_2^2]. \tag{3.19}$$

Since the unequal-arm algorithm presented above can be considered effective if $S_{\Delta C}(f) \leqslant S_N(f)$, from Eqs. (3.18), (3.19) we derive the following constraint on the accuracies δL_1, δL_2:

$$\left[\frac{\delta L_2}{L_2}-\frac{\delta L_1}{L_1}\right]^2 \leqslant \frac{S_n(f)}{S_C(f)}\frac{[L_1^2+L_2^2]}{16\pi^2 f^2 L_1^2 L_2^2}. \tag{3.20}$$

As an example application of Eq. (3.20), let us assume $\delta L_1 = -\delta L_2 \equiv \delta L$. It is easy then to derive the following inequality for $|\delta L|$:

$$|\delta L| \leqslant \frac{1}{4\pi f}\left(\frac{S_n(f)}{S_C(f)}\right)^{1/2}\frac{(L_1^2+L_2^2)^{1/2}}{|L_1+L_2|}. \tag{3.21}$$

If we specialize to $S_n(f)$ equal to the spectral density of the shot noise as given in [3], $S_C(f)$ to be the spectral density of a phase-stabilized diode-pumped Nd:YAG ring laser as also discussed in Ref. [3], and the two arm lengths $L_1 \approx L_2 = 5 \times 10^6$ km, the equation can be rewritten in the following form:

$$|\delta L| \leqslant 0.4 f^{1/3}[1+6.3\times 10^{-9} f^{-8.2/3}]^{-1/2} \text{ km}. \tag{3.22}$$

The most stringent condition on arm-length knowledge occurs, for the expected spectra given in [3], when correcting data near $f = 10^{-3}$ Hz down to the secondary noise source spectral density. At $f = 10^{-3}$ Hz, Eq. (3.22) implies that the accuracy in the arm lengths must be less than about 30 m if we require a reduction of the frequency fluctuations of the laser to the noise level identified by the photon counting statistics. Since, for the expected spectra [3], $S_n(f)$ increases quadratically with the frequency while $S_C(f)$ decreases as $f^{-2/3}$, we conclude that at higher frequencies the required accuracy is less stringent [see Eqs. (3.16), (3.17)]. At $f = 1$ Hz, for instance, we find that the required accuracy grows to about 800 m.

In relation to the accuracies derived above, it is interesting to calculate the time scales during which the arm lengths will change by an amount equal to the accuracies themselves. This identifies the minimum time required before updating the round-trip light times during the implementation of the unequal-arm algorithm.

It has been calculated by Folkner *et al.* [13] that the relative longitudinal speeds between the three pairs of spacecraft, during approximately the first year of the LISA mission [3], can be written in the following approximate form:

$$V_{i,j}(t) = V_{i,j}^{(0)} \sin\left(\frac{2\pi t}{T_{i,j}}\right), \quad (i,j)=(a,b), \quad (a,c), \quad (b,c), \tag{3.23}$$

where we have denoted by $(a,b),(a,c),(b,c)$ the three possible spacecraft pairs, $V_{i,j}^{(0)}$ is a constant velocity, and $T_{i,j}$ is the period for the pair (i,j). In Ref. [13] it has also been shown that the LISA trajectory can be selected in such a way that two of the three arms' rates of change are essentially equal during the first year of the mission. Following Ref. [13], we will assume $V_{a,b}^{(0)} = V_{a,c}^{(0)} \neq V_{b,c}^{(0)}$, with $V_{a,b}^{(0)} = 1$ m/sec, $V_{b,c}^{(0)} = 13$ m/sec, $T_{a,b} = T_{a,c} \approx 4$ months, and $T_{b,c} \approx 1$ y. From Eq. (3.23) it is easy to derive the variation of each arm length, for example $\delta L_1(t)$, as a function of the time t and the time scale δt during which it takes place:

$$\delta L_1(t) = V_{a,b}^{(0)} \sin\left(\frac{2\pi t}{T_{a,b}}\right)\delta t. \tag{3.24}$$

Equation (3.24) implies that a variation in arm length $\delta L_1 \approx 30$ m can take place during different time scales, depending on when during the mission this change takes place. For instance, if $t \ll T_{a,b}$, we find that the arm length L_1 changes

by more than its accuracy (30 m) after a time $\delta t = 6.7 \times 10^3$ sec. If however $t \simeq T_{a,b}/4$, the arm length will change by the same amount after only $\delta t \simeq 30$ sec instead.

As a final note, it is worth mentioning that, since the anticipated gravitational wave amplitude will be about seven or more orders of magnitude smaller than the relative frequency fluctuations of the laser, the Doppler measurements from each arm must be digitized with an adequate resolution. This is in order to avoid the loss of the gravitational wave signal once the subtraction of the laser noise is performed. Although this is an important point that will need to be remembered in the design of the onboard data acquisition system, it does not represent a fundamental technology challenge [3]. Furthermore, in order to have perfect synchronization of the two data streams and effectively remove the laser fluctuations, a common clock should be used during the acquisition, digitization, and recording of the two Doppler data.

IV. CONCLUSIONS

We presented a time-domain procedure for accurately canceling laser noise fluctuations in an unequal-arm one-bounce Michelson interferometer relevant to space-borne gravitational wave detectors. The method involves separately measuring the phase of the returning light relative to the phase of the transmitted light in each arm. By suitable offsetting and differencing of these two time series, the common laser noise is canceled exactly [Eq. (3.5)]. This is temporally local and contrasts with approximate cancellation techniques based on operations on Fourier transforms of long but finite durations data sets.

The effect of this procedure is to introduce a characteristic signature of a gravitational wave incident on the interferometer. In the general case, the wave is replicated 8 times in the output time series, depending on the arm lengths and the angle of arrival of the wave. We showed that our linear combination precisely cancels the laser noise, and modulates the gravitational wave signal and the secondary noise sources in the same way if the lengths of the two arms are different by only a few percent [3]. Thus the signal-to-noise ratio after applying our procedure is the same as would be expected for an equal-arm interferometer.

To cancel the laser noise to the levels of the secondary noise sources with this procedure, the arm lengths must be known with adequate accuracy. To demonstrate practicality of the method, we presented a general analysis of the required accuracy [Eqs. (3.16), (3.17), (3.20)] and used the noise spectra expected for proposed space interferometer mission to estimate required accuracy as a function of Fourier content of the signal.

Since a gravitational wave signal enters into the response of an unequal-arm interferometer in general at eight distinct times [Eq. (3.6)], the probability of detection of signal with low signal-to-noise ratios should improve. Furthermore, such a distinct time structure should enhance the angular resolution of LISA [3] for signals where the 8 pulses are resolved. These issues will be addressed in a forthcoming paper.

ACKNOWLEDGMENTS

It is a pleasure to thank Frank B. Estabrook for many useful discussions and his encouragement during this work. This research was performed at the Jet Propulsion Laboratory, California Institute of Technology, under contract with the National Aeronautics and Space Administration.

APPENDIX: FREQUENCY-DOMAIN CANCELLATION OF LASER NOISE IN UNEQUAL-ARM INTERFEROMETERS

In the main text, we gave a time-domain procedure for exactly canceling laser noise fluctuations in an unequal arm Michelson interferometer while preserving the gravitational wave (GW) signal. A procedure for cancellation of laser noise involving operations on the Fourier transforms of the data from each arm was previously presented in [5]. This frequency-domain (FD) method cancels the laser noise exactly in the limit where the duration of the data set goes to infinity. For a finite data set, however, the FD cancellation method is not exact. For the very precise cancellation required for a gravitational wave detector in space (140–200 dB, depending on Fourier frequency), the FD procedure requires impractically long data sets. In this appendix we briefly restate the FD cancellation argument, derive an analytical expression for the degree of cancellation of the FD method as a function of arm lengths, duration of the data set, and Fourier frequency [Eq. (A24)], compare this analytical result with computer simulations, and discuss practical implications for space-borne laser interferometer GW experiments.

1. Frequency-domain method

The FD method is described in detail in [5]. Briefly, the difference between the phase (or frequency) of the transmitted laser signal at time t and the laser phase at a ''two-way light time'' earlier is recorded separately for each arm of the interferometer. This is done over some observing interval, *T*. Using the same notation as in the main text, these two time series are

$$y_1(t) = h_1(t) + C(t - 2L_1) - C(t) + n_1(t), \tag{A1}$$

$$y_2(t) = h_2(t) + C(t - 2L_2) - C(t) + n_2(t), \tag{A2}$$

where L_1 and L_2 are the arm lengths of the interferometer (in units of time, $c = 1$), $h_1(t)$, $h_2(t)$ are the GW signal amplitudes, $C(t)$ is the laser noise process, and $n_1(t)$, $n_2(t)$ are all other noises entering the data. $C(t)$ totally dominates n_1 and n_2 ($\sim 10^7$ or more times larger in amplitude); so the objective is to cancel $C(t)$ to a level smaller than the other noise sources while preserving the GW signal.

The FD approach is first to Fourier transform y_1 and y_2. Conceptually this is a true Fourier transform (i.e., infinite limits of integration); in practice it is a transform over a finite interval set by practical considerations. Let $\tilde{y}_i(f)$ be the sample Fourier transform of the series $y_i(t)$. Using the shift

theorem for Fourier transforms [12] one can use the data in, e.g., arm 2 to solve for $\tilde{C}(f)$, the Fourier transform of $C(t)$:

$$\tilde{C}(f)=\frac{\tilde{y}_2(f)}{[1-e^{-4\pi i f L_2}]}. \tag{A3}$$

Given this estimate of $\tilde{C}(f)$ one can correct the data in the other arm for laser fluctuations. The Fourier transform of the corrected data is then

$$\tilde{y}_1(f)-\tilde{y}_2(f)\frac{[e^{4\pi i f L_1}-1]}{[e^{4\pi i f L_2}-1]}. \tag{A4}$$

The ensemble average of the square of this quantity is the power spectrum of the FD corrected data; as shown in [5] it goes to zero [except at the poles in Eq. (A4), i.e. $f=0$ and the time-travel resonances of arm 2] if there is laser noise only and if the data set is infinitely long. This FD approach preserves a GW signal. Equation (A4) is the essential result of the FD-correction approach.

2. Performance of the frequency domain approach for finite data sets

In a finite-duration experiment, the FD cancellation is not exact. The degree to which the FD method cancels the laser noise depends on the duration of the Fourier transforms used, how the data are ''windowed'' [11] in the time domain before estimating the Fourier transform, the interferometer arm lengths, and the Fourier frequency considered.

Define $\tilde{y}_1(f)$ as the ''forward'' Fourier transform of the Doppler data $y_1(t)$ calculated over the interval $T\equiv 2\tau$:

$$\tilde{y}_1(f)\equiv\int_{-\tau}^{\tau} y_1(t)e^{2\pi i f t}dt. \tag{A5}$$

From the Fourier theorem, the inverse Fourier transform, $y_1(t)$, is given by

$$y_1(t)\equiv\int_{-f_c}^{+f_c}\tilde{y}_1(f)e^{-2\pi i f t}df, \tag{A6}$$

where f_c is the Nyquist frequency cutoff. For a space-based interferometer, for instance, f_c might be 0.5 Hz. Note that if we substitute Eq. (A6) into Eq. (A5) we get

$$\tilde{y}_1(f)=\int_{-\tau}^{\tau}\int_{-f_c}^{+f_c}\tilde{y}_1(f')e^{2\pi i(f-f')t}df'dt, \tag{A7}$$

which, after integration with respect to time, becomes

$$\tilde{y}_1(f)=\int_{-f_c}^{+f_c}\tilde{y}_1(f')\left[\frac{\sin[\pi(f-f')T]}{\pi(f-f')}\right]df'. \tag{A8}$$

Since the function inside the squared brackets is one of the approximations to the Dirac delta function, we conclude that Eq. (A8) becomes an identity, in agreement with the definitions of forward and backward Fourier transforms given in Eqs. (A5), (A6).

To minimize spectral leakage [11], it is necessary to premultiply the time-domain data sets by a window function, $W(t)$, before taking Fourier transforms. If $Y_1(t)\equiv y_1(t)W(t)$, and $Y_2(t)\equiv y_2(t)W(t)$, the finite-duration windowed Fourier transform of, e.g., $Y_1(t)$, is equal to

$$\tilde{Y}_1(f)=\tilde{H}_1(f)+\int_{-\tau}^{\tau}[C(t-2L_1)-C(t)]W(t)e^{2\pi i f t}dt + \tilde{N}_1(f), \tag{A9}$$

where $\tilde{H}_1(f)$, $\tilde{N}_1(f)$ are the Fourier transforms of $h_1(t)W(t)$, $n_1(t)W(t)$ respectively. Since $C(t)$, $W(t)$ can be written in terms of their inverse Fourier transforms, after some simple algebra we can rewrite Eq. (A9) as

$$\tilde{Y}_1(f)=\tilde{H}_1(f)+\int_{-\tau}^{\tau}\int_{-f_c}^{f_c}\int_{-f_c}^{f_c}\tilde{C}(f')[e^{4\pi i f' L_1}-1] \times\tilde{W}(f'')e^{2\pi i(f-f'-f'')t}dtdf'df''+\tilde{N}_1(f). \tag{A10}$$

If we interchange the integration symbols, and integrate with respect to time, Eq. (A10) becomes

$$\tilde{Y}_1(f)=\tilde{H}_1(f)+\int_{-f_c}^{f_c}\int_{-f_c}^{f_c}\tilde{C}(f')[e^{4\pi i f' L_1}-1]\tilde{W}(f'') \times\left[\frac{\sin[\pi(f-f'-f'')T]}{\pi(f-f'-f'')}\right]df'df''+\tilde{N}_1(f). \tag{A11}$$

By further integrating Eq. (A11) with respect to f'' we obtain

$$\tilde{Y}_1(f)=\tilde{H}_1(f)+\int_{-f_c}^{f_c}\tilde{C}(f')[e^{4\pi i f' L_1}-1]\tilde{W}(f-f')df' + \tilde{N}_1(f). \tag{A12}$$

If $W(t)$ is the Parzen (triangular) window [11], its Fourier transform is

$$\tilde{W}(f)=\tau\left[\frac{\sin(\pi f\tau)}{\pi f\tau}\right]^2, \tag{A13}$$

and we can rewrite Eq. (A12) as follows:

$$\tilde{Y}_1(f)=\tilde{H}_1(f)+\tau\int_{-f_c}^{f_c}\tilde{C}(f')[e^{4\pi i f' L_1}-1] \times\left[\frac{\sin[\pi(f-f')\tau]}{\pi(f-f')\tau}\right]^2 df'+\tilde{N}_1(f). \tag{A14}$$

If we now make the change of variable $\pi(f-f')\tau=\eta$, Eq. (A14) becomes

$$\tilde{Y}_1(f)=\tilde{H}_1(f)+\frac{1}{\pi}\int_{\pi\tau(f-f_c)}^{\pi\tau(f+f_c)}\tilde{C}\left(f-\frac{\eta}{\pi\tau}\right)[e^{4\pi i(f-\eta/\pi\tau)L_1}-1]\times\left[\frac{\sin(\eta)}{\eta}\right]^2 d\eta+\tilde{N}_1(f). \tag{A15}$$

Since the integrand in Eq. (A15) decays as η^{-2}, the major contribution to the integral will come from a few cycles around zero. This implies that the integrand in Eq. (A15) can be written in the following approximate form:

$$\tilde{Y}_1(f)=\tilde{H}_1(f)+\frac{1}{\pi}\int_{\pi\tau(f-f_c)}^{\pi\tau(f+f_c)}\tilde{C}\left(f-\frac{\eta}{\pi\tau}\right)\times\left[e^{4\pi ifL_1}\left(1-\frac{4iL_1\eta}{\tau}\right)-1\right]\left[\frac{\sin(\eta)}{\eta}\right]^2 d\eta+\tilde{N}_1(f). \tag{A16}$$

After some further algebra, Eq. (A16) can be rewritten as follows:

$$\tilde{Y}_1(f)=\tilde{H}_1(f)+\frac{1}{\pi}\int_{\pi\tau(f-f_c)}^{\pi\tau(f+f_c)}\tilde{C}\left(f-\frac{\eta}{\pi\tau}\right)\times\left[\frac{\sin(\eta)}{\eta}\right]^2 d\eta[e^{4\pi ifL_1}-1]-\frac{4iL_1}{\pi\tau}e^{4\pi ifL_1}\int_{\pi\tau(f-f_c)}^{\pi\tau(f+f_c)}\tilde{C}\left(f-\frac{\eta}{\pi\tau}\right)\left[\frac{\sin^2(\eta)}{\eta}\right]d\eta+\tilde{N}_1(f), \tag{A17}$$

and similarly we can write the corresponding equation for the Fourier transform of the windowed Doppler data measured with arm 2. We point out that in Eq. (A17) the second integral goes to zero as the integration time goes to infinity; however, for any finite time of integration the transfer function of the frequency fluctuations of the laser into the Doppler observables will not have the ideal analytic forms

$$e^{4\pi ifL_{(1,2)}}-1. \tag{A18}$$

If we implement the FD technique proposed in [5] for removing the laser noise, we get

$$\tilde{Y}_1(f)-\tilde{Y}_2(f)\frac{[e^{4\pi ifL_1}-1]}{[e^{4\pi ifL_2}-1]}=[\tilde{H}_1(f)+\tilde{N}_1(f)]-[\tilde{H}_2(f)+\tilde{N}_2(f)]\frac{[e^{4\pi ifL_1}-1]}{[e^{4\pi ifL_2}-1]}+\frac{4i}{\pi\tau}\left[L_2e^{4\pi ifL_2}\frac{[e^{4\pi ifL_1}-1]}{[e^{4\pi ifL_2}-1]}-L_1e^{4\pi ifL_1}\right]\int_{\pi\tau(f-f_c)}^{\pi\tau(f+f_c)}\tilde{C}\left(f-\frac{\eta}{\pi\tau}\right)\left[\frac{\sin^2(\eta)}{\eta}\right]d\eta. \tag{A19}$$

The last term on the right-hand-side of Eq. (A19) can be rewritten as

$$\tilde{Y}_C(f)\equiv\left(\frac{2}{\pi\tau\sin(2\pi fL_2)}\right)e^{2\pi if(2L_1+L_2)}[L_2-L_1+L_1e^{-4\pi ifL_2}-L_2e^{-4\pi ifL_1}]\int_{\pi\tau(f-f_c)}^{\pi\tau(f+f_c)}\tilde{C}\left(f-\frac{\eta}{\pi\tau}\right)\times\left[\frac{\sin^2(\eta)}{\eta}\right]d\eta. \tag{A20}$$

If we take the modulus squared and the ensemble average ($\langle\cdots\rangle$) of the left- and right-hand sides of Eq. (A20), we get

$$\langle|\tilde{Y}_C(f)|^2\rangle\equiv\left(\frac{2}{\pi\tau\sin(2\pi fL_2)}\right)^2\{(L_2-L_1)^2+L_1^2+L_2^2-2L_1L_2\cos[4\pi f(L_2-L_1)]+2(L_2-L_1)L_1\cos(4\pi fL_2)-2(L_2-L_1)L_2\cos(4\pi fL_1)\}\int_{\pi\tau(f-f_c)}^{\pi\tau(f+f_c)}\int_{\pi\tau(f-f_c)}^{\pi\tau(f+f_c)}\left\langle\tilde{C}\left(f-\frac{\eta}{\pi\tau}\right)\tilde{C}^*\left(f-\frac{\eta'}{\pi\tau}\right)\right\rangle\left[\frac{\sin^2(\eta)}{\eta}\right]\left[\frac{\sin^2(\eta')}{\eta'}\right]d\eta d\eta'. \tag{A21}$$

Assuming $C(t)$ is a stationary random process with power spectral density $S_C(f)$, we can rewrite Eq. (A21) as follows:

$$\langle|\tilde{Y}_C(f)|^2\rangle\equiv\left(\frac{2}{\pi\tau\sin(2\pi fL_2)}\right)^2\{(L_2-L_1)^2+L_1^2+L_2^2-2L_1L_2\cos[4\pi f(L_2-L_1)]+2(L_2-L_1)L_1\cos(4\pi fL_2)-2(L_2-L_1)L_2\cos(4\pi fL_1)\}\int_{\pi\tau(f-f_c)}^{\pi\tau(f+f_c)}\int_{\pi\tau(f-f_c)}^{\pi\tau(f+f_c)}S_C\left(f-\frac{\eta}{\pi\tau}\right)\delta(\eta-\eta')\left[\frac{\sin^2(\eta)}{\eta}\right]\left[\frac{\sin^2(\eta')}{\eta'}\right]d\eta d\eta', \tag{A22}$$

which then becomes

$$\langle|\tilde{Y}_C(f)|^2\rangle \equiv \left(\frac{4}{\pi T \sin(2\pi f L_2)}\right)^2 \{(L_2-L_1)^2+L_1^2+L_2^2-2L_1L_2\cos[4\pi f(L_2-L_1)]+2(L_2-L_1)L_1\cos(4\pi f L_2)$$
$$-2(L_2-L_1)L_2\cos(4\pi f L_1)\}\int_{\pi\tau(f-f_c)}^{\pi\tau(f+f_c)} S_C\left(f-\frac{\eta}{\pi\tau}\right)\left[\frac{\sin^4(\eta)}{\eta^2}\right]d\eta, \tag{A23}$$

where the identity $T=2\tau$ has been used. Since the power spectral density of the frequency fluctuations of a stabilized laser is a smooth function of the frequency, the major contribution to the integral will come from a few cycles around zero. This implies that we can treat the power spectral density $S_C(f)$ essentially as a constant in doing this integration, and rewrite Eq. (A23) as

$$\langle|\tilde{Y}_C(f)|^2\rangle = \frac{16S_C(f)F(L_1,L_2,f)}{\pi^2T^2}\int_{\pi\tau(f-f_c)}^{\pi\tau(f+f_c)}\left[\frac{\sin^4(\eta)}{\eta^2}\right]d\eta, \tag{A24}$$

where $F(L_1,L_2,f)$ is

$$F(L_1,L_2,f)=\frac{1}{\sin^2(2\pi f L_2)}\{(L_2-L_1)^2+L_1^2+L_2^2$$
$$-2L_1L_2\cos[4\pi f(L_2-L_1)]$$
$$+2(L_2-L_1)L_1\cos(4\pi f L_2)$$
$$-2(L_2-L_1)L_2\cos(4\pi f L_1)\}. \tag{A25}$$

Equation (A24) is the main result of this appendix. For a finite-duration experiment, it expresses the degree of FD cancellation of the laser noise as a function of the two arm lengths, the spectrum of the laser noise, the experiment duration, and Fourier frequency.

3. Simulation

We verified this formula via simulated time series of various durations, various arm lengths, and various arm length differences. To make a more direct comparison with the FD method in [5], these simulations were done in terms of phase rather than fractional frequency difference. Figure 4 shows one of these simulations, the parameters of which closely follow those used in [5]. We simulated white laser phase noise with two-sided spectral density $S_\phi(f)=2.5\times10^7$ rad^2/Hz (i.e., rms phase of 5000 radians in a 1 Hz band) and white ''other'' noise (independent in each arm and with spectral density much smaller than the laser noise [5]). From the simulated time series of laser noise we formed the time series of laser phase noise differences, $p(t-2L_i)-p(t)$, for each arm. A simulated sinusoidal gravitational wave signal was injected at $f_0=0.1$ Hz, with amplitude $h_0=10^{-20}$. The gravitational wave was assumed incident normally onto the plane of the interferometer so that the phase data in each arm has two ''pulses'' separated by the two-way light travel time in that arm [2]. As in [5] the signal was added to one arm and subtracted from the other. The two-way light times used were $2L_1=16.6875$ sec and $2L_2=16.71875$ sec (i.e., they differed by 1/32 of a second) and were assumed to be known exactly. Thus the observable time series of the two arms were

$$z_1(t)=s_1(t)+p(t-2L_1)-p(t)+\lambda_1(t), \tag{A26}$$

$$z_2(t)=s_2(t)+p(t-2L_2)-p(t)+\lambda_2(t), \tag{A27}$$

where

$$s_1(t)=\frac{1}{2}h_0\left(\frac{3\times10^{14}\ \text{Hz}}{f_0}\right)\{\cos[2\pi f_0(t-2L_1)]$$
$$-\cos(2\pi f_0 t)\}, \tag{A28}$$

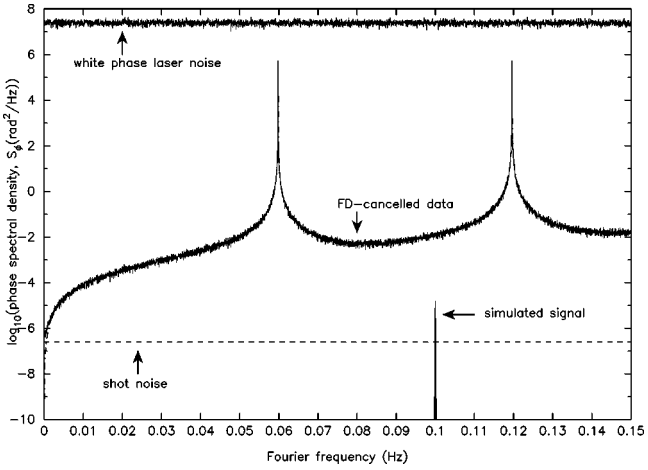

FIG. 4. Phase spectra of simulated laser noise illustrating the performance of the frequency-domain cancellation procedure for unequal arm interferometers, as discussed in the Appendix. Upper curve: spectrum of raw laser phase noise (assumed white with spectral level 2.5×10^7 rad^2/Hz). Lower curve: spectrum of frequency-domain canceled noise for parameters $2L_1=16.6875$ sec, $2L_2=16.71875$ sec, duration of data $=2^{15}$ sec. Thirty realizations of each spectrum were averaged to reduce estimation error and more clearly illustrate spectral shapes. Also plotted as a dot-dashed line is the model prediction [Eq. (A24)]. Dashed line: spectral density of white ''shot'' noise added to each arm. The spectral line is a FD-cancellation response of interferometer to gravitational wave incident normal to the plane of the interferometer with $f_0=0.1$ Hz. For these arm lengths, the FD-cancellation method would require long transform lengths (about 6 months) to suppress the laser noise by 140 dB in the band $10^{-2}-10^{-4}$ Hz.

$$s_2(t) = -\frac{1}{2}h_0\left(\frac{3\times 10^{14}\ \text{Hz}}{f_0}\right)\{\cos[2\pi f_0(t-2L_2)] - \cos(2\pi f_0 t)\}. \quad \text{(A29)}$$

The minus sign on the right-hand side of the equation for s_2 reflects the quadrupolar nature of the gravitational wave signal [8], the optical carrier frequency ($\nu_0 = 3\times 10^{14}$ Hz) is appropriate for a 1 μm laser [3], and the frequency fluctuation $y(t) = \Delta\nu/\nu_0$ has been integrated to get the associated phase fluctuation $z(t)$. The ''other'' phase noises, λ_1, λ_2 in Eqs. (A26) and (A27) were taken to be white phase noise, independent in each arm, and with spectral density 14 orders of magnitude smaller than that of the laser phase noise [5]. [The crucial difference between our simulation and that done in [5] is that the laser phase noise time series, $p(t)$, was required in [5] to be periodic with the same period as that of the finite Fourier transform. This periodicity condition—which would not be satisfied in a real observation—forces the phase difference series in each arm, $p(t-2L_i)-p(t)$, to have the idealized analytic form of Eq. (A18), even for a *finite* duration rectangular windowed Fourier transform. Thus the simulation in [5] erroneously appeared to achieve exact laser-noise cancellation even for a finite duration data set.]

A simulated duration of $T = 2^{15}$ sec was used to compute Fourier transforms. All time series were multiplied by a triangle window function prior to being discrete-Fourier transformed. Figure 4 shows spectra averaged over 30 realizations of the simulated processes (to reduce estimation error). Shown in the figure are the raw laser noise spectrum and the spectrum of the FD-canceled noise process. The noise level of the ''other'' noise processes (140 dB below the laser phase noise) is indicated as a dashed line. The spectrum of the monochromatic signal with $h_0 = 10^{-20}$, passed through the interferometer response and with frequency resolution appropriate for $T = 2^{15}$ sec, is also indicated. Our analytical result [Eq. (A24)] is overplotted as a dot-dashed line on the FD-canceled spectrum (although the model curve is difficult to see because of the excellent agreement.) For these parameters, the FD method fails to cancel the laser noise to desired levels over essentially all of the band.

4. Implications for space-borne gravitational wave interferometers

FD cancellation presents conflicting requirements: the data duration, T, must be long enough to get 140–200 dB suppression of the laser noise (depending on Fourier frequency), but simultaneously (at least in the FD approach as formulated to date) short enough so that the arm lengths are sensibly constant. Using as an example the published parameters of the proposed LISA mission [3], the arms can be up to 3% different and the peak rate of change of an arm will be about 13 m/sec. Taking the arm lengths to be 1% percent different with $2L_1 = 33$ sec and $2L_2 = 33.3$ sec and requiring at least 140 dB suppression in the Fourier band 10^{-4}–10^{-2} Hz, requires [Eq. (A24)] a data duration of $T \approx 6$ months. On this time scale the arms will change by much more than the tolerance derived for the FD method [5] and in the main text of this paper. Restricting the time duration of the FD method to a value where the arm lengths do not change significantly [13,14] results in insufficient suppression of the laser noise.

[1] M. Tinto and F. B. Estabrook, Phys. Rev. D **52**, 1749 (1995).

[2] F. B. Estabrook and H. D. Wahlquist, Gen. Relativ. Gravit. **6**, 439 (1975).

[3] ''LISA (Laser Interferometer Space Antenna): An international project in the field of Fundamental Physics in Space,'' Pre-Phase A Report No. MPQ 233, Max-Planck-Institute für Quantenoptic, Garching bei München, 1998.

[4] D. Shoemaker, R. Schilling, L. Schnupp, W. Winkler, K. Maischberger, and A. Rüdiger, Phys. Rev. D **38**, 423 (1988).

[5] G. Giampieri, R. W. Hellings, M. Tinto, and J. E. Faller, Opt. Commun. **123**, 669 (1996).

[6] F. B. Estabrook, Gen. Relativ. Gravit. **17**, 719 (1985).

[7] H. D. Wahlquist, Gen. Relativ. Gravit. **19**, 1101 (1987).

[8] S. V. Dhurandhar and M. Tinto, Mon. Not. R. Astron. Soc. **234**, 662 (1988).

[9] P. W. McNamara, H. Ward, J. Hough, and D. Robertson, Class. Quantum Grav. **14**, 1543 (1997).

[10] Y. Gürsel and M. Tinto, Phys. Rev. D **40**, 3884 (1989).

[11] G. M. Jenkins and D. G. Watts, *Spectral Analysis and Its Applications* (Holden-Day, San Francisco, 1968).

[12] R. Bracewell, *The Fourier Transform and Its Applications* (McGraw-Hill, New York, 1965).

[13] W. M. Folkner, F. Hechler, T. H. Sweetser, M. A. Vincent, and P. L. Bender, Class. Quantum Grav. **14**, 1543 (1997).

[14] M. Tinto, Phys. Rev. D **58**, 102001 (1998).